Periodic Signal Modeling Based on Liénard's Equation*

E. Abd-Elrady, T. Söderström, T. Wigren

Systems and Control, Dept. of Information Technology, Uppsala University,
P.O. Box 337, SE-751 05 Uppsala, Sweden.

August 11, 2003

Abstract

The problem of modeling periodic signals is considered. The approach taken here is motivated by the well known theoretical results on the existence of periodic orbits for Liénard systems and previous results on modeling periodic signals by means of second order nonlinear ordinary differential equations (ODEs). The approach makes use of the appropriate conditions imposed on the polynomials of a Liénard system to guarantee the existence of a unique and stable limit cycle. These conditions reduce the number of parameters required to generate accurate models for periodic signals.

Keywords: Identification, Liénard's equation, Limit cycle, Nonlinear systems, Periodic orbit.

1 Introduction

There is a quite substantial literature on modeling of periodic signals, which is considered to be a fundamental problem in many applications. Examples include vibration analysis, speech synthesis, overtone analysis in power networks and measurement of linearity in electronic power amplifiers, see [1-4].

Many systems that generate periodic signals are best described by second order nonlinear ordinary differential equations (ODEs) with polynomial right hand sides. Examples include tunnel diodes, pendulums, negative-resistance oscillators and biochemical reactors, see [5-8].

In [9-11] periodic signals were modeled by introducing a polynomial parameterization of the right hand side of a general second order ODE, and by defining the periodic signal to be modeled as a function of the states of this ODE. Estimators based on a Kalman filter (KF) and an extended Kalman filter (EKF) were developed in [9]. A least squares (LS) estimation algorithm was derived in [10]. Also, an estimation algorithm based on the Markov estimate was introduced in [11].

*This work was supported in part by Swedish Research Council for Engineering Sciences under contract 98-654.

In the early days of nonlinear dynamics, it was found that many oscillating circuits can be modeled by the following second order differential equation known as *Liénard's equation*, see [6, 7, 12],

$$\ddot{y} + f(y)\dot{y} + g(y) = 0. \tag{1}$$

Liénard's equation can be interpreted mechanically as the equation of motion for a unit mass subject to a nonlinear damping force $-f(y)\dot{y}$ and a nonlinear restoring force $-g(y)$. This equation is a generalization of the *Van der Pol* oscillator given by

$$\ddot{y} + \mu(y^2 - 1)\dot{y} + y = 0. \tag{2}$$

for which $f(y) = \mu(y^2 - 1)$ and $g(y) = y$.

Choosing the state variables as

$$\begin{pmatrix} x_1 \\ x_2 \end{pmatrix} = \begin{pmatrix} y(t) \\ \dot{y}(t) \end{pmatrix} \tag{3}$$

Liénard's equation is equivalent to the system

$$\dot{x}_1 = x_2 \tag{4}$$

$$\dot{x}_2 = -g(x_1) - f(x_1)x_2 \tag{5}$$

which is known as the *Liénard's system.*

Applications of Liénard's equation can be found in many important examples. Examples include chemical reactions, growth of a single species, predator-prey systems and vibration analysis, see [13].

In this paper Liénard's equation is used to model periodic signals following the approach introduced in [9-11]. The conditions that guarantee the existence of periodic orbits for Liénard systems, see [6, 7, 12], are used to reduce the number of parameters required to model periodic signals. This is expected to give significantly better parameter accuracy as compared to the approach used in [9-11] in case the modeled signal fulfills Liénard's equation.

The paper is organized as follows. Section 2 introduces the details on the model. Section 3 analyzes the conditions imposed on the model to achieve the reduction in the parameters to be estimated. Section 4 presents a comparative simulation study between the approach taken in this paper and the approach of [9-11]. Conclusions appear in Section 5.

2 The model

2.1 Measurements

The starting point is the discrete time measured signal $z(kT_S)$, where

$$z(kT_S) = y(kT_S) + e(kT_S) \tag{6}$$

Here $y(t)$ is the continuous time signal to be modeled, $y(kT_S)$ its sampled value, $e(kT_S)$ is the discrete time measurement noise and T_S the sampling interval. It is assumed here that $y(t)$ is periodic, *i.e.*

$\mathcal{C}1$: $y(t+T) = y(t),\ \forall t \in R, 0 < T < \infty$.

Furthermore, $e(kT_S)$ is assumed to be zero mean Gaussian white noise, *i.e.*

$\mathcal{C}2$: $e(kT_S) \in N(0, \sigma^2),\ \mathrm{E}[e(kT_S)e(kT_S + jT_S)] = \delta_{j,0}\sigma^2$.

where E is the expectation operator.

2.2 Model Structures

The work done in [9-11] is based on modeling the signal $y(t)$ by means of an unknown parameter vector $\tilde{\boldsymbol{\theta}}$ and an ODE of order two, *i.e.*

$$\begin{pmatrix} \dot{x}_1 \\ \dot{x}_2 \end{pmatrix} = \begin{pmatrix} x_2(t) \\ F(x_1(t), x_2(t), \tilde{\boldsymbol{\theta}}) \end{pmatrix} \tag{7}$$

$$y(t) = \begin{pmatrix} 1 & 0 \end{pmatrix} \begin{pmatrix} x_1(t) \\ x_2(t) \end{pmatrix}. \tag{8}$$

It is proved rigorously in [14] that an ODE of order 2 is sufficient to model a large class of periodic signals. The right hand side of the second state equation of (7) is expanded in terms of known basis functions. Hence $F(x_1(t), x_2(t), \tilde{\boldsymbol{\theta}})$ is taken as a truncated superposition of these functions. In case of a polynomial model, a suitable parameterization is

$$F(x_1(t), x_2(t), \tilde{\boldsymbol{\theta}}) = \sum_{l=0}^{L} \sum_{m=0}^{M} \tilde{\theta}_{l,m} x_1^l(t) x_2^m(t), \tag{9}$$

$$\tilde{\boldsymbol{\theta}} = \begin{pmatrix} \tilde{\theta}_{0,0} \cdots \tilde{\theta}_{0,M} & \tilde{\theta}_{1,0} \cdots \tilde{\theta}_{1,M} & \cdots & \tilde{\theta}_{L,0} \cdots \tilde{\theta}_{L,M} \end{pmatrix}^T. \tag{10}$$

In this paper a Liénard model (4)-(5) is used for modeling periodic signals. Then the state space model (7)-(8) becomes

$$\begin{pmatrix} \dot{x}_1 \\ \dot{x}_2 \end{pmatrix} = \begin{pmatrix} x_2(t) \\ -g(x_1, \boldsymbol{\theta_1}) - f(x_1, \boldsymbol{\theta_2}) x_2 \end{pmatrix} \tag{11}$$

$$y(t) = \begin{pmatrix} 1 & 0 \end{pmatrix} \begin{pmatrix} x_1(t) \\ x_2(t) \end{pmatrix} \tag{12}$$

$$\boldsymbol{\theta} = \begin{pmatrix} \boldsymbol{\theta_1}^T & \boldsymbol{\theta_2}^T \end{pmatrix}^T. \tag{13}$$

Also here $g(x_1, \boldsymbol{\theta_1})$ and $f(x_1, \boldsymbol{\theta_2})$ are parameterized using (scalar) polynomial models

$$g(x_1, \boldsymbol{\theta_1}) = \sum_{l_1=1}^{L_1} \theta_{1,l_1} x_1^{l_1}(t) \tag{14}$$

$$f(x_1, \boldsymbol{\theta_2}) = \sum_{l_2=0}^{L_2} \theta_{2,l_2} x_1^{l_2}(t) \tag{15}$$

Needless to say, the model (11) can be seen as a special case of the general case (7).

Remark 1. In nonlinear systems theory, it is usually assumed that the system has an equilibrium at the origin without any loss of generality because any equilibrium point can be shifted to the origin via a change of variables. This is the reason why the constant term is dropped in $g(x_1, \boldsymbol{\theta_1})$. *i.e.*, $\theta_{1,0} = 0$ in (14), see [5].

The suggested model in (11) has been widely studied, see [6, 7, 12], to investigate the existence of limit cycles and study their stability. The celebrated *Liénard's theorem* [12] imposes appropriate assumptions on $g(x_1, \boldsymbol{\theta_1})$ and $f(x_1, \boldsymbol{\theta_2})$ to guarantee the existence of a unique, stable periodic orbit. These assumptions are studied in Section 3 to reduce the number of parameters required to model periodic signals compared to the approach of [9-11], which is based on the more general model (7).

2.3 Discretization

In order to formulate complete discrete time models, the continuous time ODE model (11) needs to be discretized. This is done by exploiting an Euler forward numerical integration scheme. For simplicity, the discretization interval is selected to be equal to the sampling period T_S, resulting in

$$x_1(kT_S + T_S) = x_1(kT_S) + T_S x_2(kT_S) \tag{16}$$

$$x_2(kT_S + T_S) = x_2(kT_S) - T_S \sum_{l_1=1}^{L_1} \theta_{1,l_1} x_1^{l_1}(kT_S) - T_S \left(\sum_{l_2=0}^{L_2} \theta_{2,l_2} x_1^{l_2}(kT_S) \right) x_2(kT_S). \tag{17}$$

Remark 2. In the following, for notational convenience the dependence on T_S is omitted assuming T_S equal to one time unit. This means that an integer k can be used as the time variable.

The model (16)-(17) can then be compactly written as

$$x_1(k+1) - x_1(k) = x_2(k) \tag{18}$$

$$x_2(k+1) - x_2(k) = -\, \boldsymbol{\phi}^T(x_1(k), x_2(k))\, \boldsymbol{\theta} \tag{19}$$

where

$$\boldsymbol{\phi}^T(x_1(k), x_2(k)) = \begin{pmatrix} x_1(k) & \cdots & x_1^{L_1}(k) & x_2(k) & \cdots & x_1^{L_2}(k)x_2(k) \end{pmatrix} \tag{20}$$

$$\boldsymbol{\theta} = \begin{pmatrix} \theta_{1,1} & \cdots & \theta_{1,L_1} & \theta_{2,0} & \cdots & \theta_{2,L_2} \end{pmatrix}^T. \tag{21}$$

For comparison, discretizing the second state equation of (7) results in

$$x_2(k+1) - x_2(k) = \tilde{\boldsymbol{\phi}}^T(x_1(k), x_2(k))\, \tilde{\boldsymbol{\theta}} \tag{22}$$

where

$$\begin{aligned} &\tilde{\boldsymbol{\phi}}^T(x_1(k), x_2(k)) = \\ &\quad \begin{pmatrix} 1 & x_2(k) \cdots x_2^M(k) & x_1(k) \cdots x_1(k)\, x_2^M(k) & \cdots & x_1^L(k) \cdots x_1^L(k)\, x_2^M(k) \end{pmatrix} \end{aligned} \tag{23}$$

and the parameter vector $\tilde{\boldsymbol{\theta}}$ is given by (10). Note the sign difference in the right hand side of (19) and (22) and that both (19) and (22) can be seen as linear regression models.

2.4 Algorithms

In order to derive different estimation schemes based on the model (18)-(19) there are at least two choices. The first choice is to formulate the model in a linear regression form using the measured data and to use the following two approximations, *cf.* (3).

1. As $y = x_1$ is not known, use the estimate

$$\widehat{x}_1(k) = z(k). \tag{24}$$

2. As $\dot{y} = x_2$ is not known, use the estimate

$$\widehat{x}_2(k) = z(k+1) - z(k). \tag{25}$$

   Recall that, due to the notational convention, (25) in fact means

$$\widehat{x}_2(kT_S) = \frac{z(kT_S + T_S) - z(kT_S)}{T_S}. \tag{26}$$

Remark 3. More general differentiating filters than (25) can be used. Reasonable differentiating filters are of the form

$$\tilde{H}(q) = (q-1)\ H(q) \tag{27}$$

with $H(q)$ a low pass filter ($qz(k) = z(k+1)$) of unity static gain. See [15] for more details about differentiating filters.

Once the model is formulated in the linear regression form, a number of different estimation algorithms based on the Kalman filter [9], the least squares estimate [10] and the Markov estimate [11] can be developed from the model (18)-(19).

Another choice is to estimate the states $x_1(k)$ and $x_2(k)$ in addition to the parameter vector $\boldsymbol{\theta}$ using the EKF as done in [9]. In this case the regression vector $\boldsymbol{\phi}^T(x_1(k), x_2(k))$ is built up from the estimated states $\widehat{x}_1(k)$ and $\widehat{x}_2(k)$ rather than directly from measured data as in (24) and (25).

3 Model parameterization using Liénard's theorem

In this section the model assumptions introduced in Liénard's theorem [12] are considered and exploited. The theorem reads as follows.

Theorem 1. (Liénard's theorem) Suppose that $f(y)$ and $g(y)$ satisfy the following conditions:

$\mathcal{C}3:$ $f(y)$ and $g(y)$ are continuously differentiable for all y;

$\mathcal{C}4:$ $g(-y) = -g(y)\ \forall\ y$ (*i.e.*, $g(y)$ is an *odd* function);

$\mathcal{C}5:$ $g(y) > 0$ for $y > 0$;

$\mathcal{C}6:$ $f(-y) = f(y)\ \forall\ y$ (*i.e.*, $f(y)$ is an *even* function);

$\mathcal{C}7$: The odd function $F(y) = \int_0^y f(u)du$ has exactly *one* positive zero at $y = a$, is negative for $0 < y < a$, is positive and nondecreasing for $y > a$, and $F(y) \to \infty$ as $y \to \infty$.

Then the system (4)-(5) has a *unique*, *stable* limit cycle surrounding the origin in the phase plane.

Proof. See [6, 7].

Remark 4. The assumptions on $g(y)$ mean that the restoring force acts like an ordinary spring and tends to reduce any displacement. On the other hand, the assumptions on $f(y)$ imply that the damping is negative at small $|y|$ and positive at large $|y|$. Since small oscillations are amplified and large oscillations are damped, the system tends to settle into a self-sustained oscillation of some intermediate amplitude.

Applying conditions $\mathcal{C}4$ and $\mathcal{C}6$, the models (14) and (15) take the form

$$g(x_1, \bar{\boldsymbol{\theta}}_{\mathbf{1}}) = \sum_{l_1=0}^{\bar{L}_1} \bar{\theta}_{1,l_1} x_1^{2l_1+1}(t) \tag{28}$$

$$f(x_1, \bar{\boldsymbol{\theta}}_{\mathbf{2}}) = \sum_{l_2=0}^{\bar{L}_2} \bar{\theta}_{2,l_2} x_1^{2l_2}(t) \tag{29}$$

where

$$\begin{aligned} \bar{\boldsymbol{\theta}} &= \begin{pmatrix} \bar{\boldsymbol{\theta}}_1^T & \bar{\boldsymbol{\theta}}_2^T \end{pmatrix}^T \\ &= \begin{pmatrix} \bar{\theta}_{1,0} & \cdots & \bar{\theta}_{1,\bar{L}_1} & \bar{\theta}_{2,0} & \cdots & \bar{\theta}_{2,\bar{L}_2} \end{pmatrix}^T \end{aligned} \tag{30}$$

and

$$\bar{L}_1 = \frac{L_1 - 1}{2} \tag{31}$$

$$\bar{L}_2 = \frac{L_2}{2}. \tag{32}$$

Hence (19) becomes

$$x_2(k+1) - x_2(k) = -\, \bar{\boldsymbol{\phi}}^T(x_1(k), x_2(k))\, \bar{\boldsymbol{\theta}} \tag{33}$$

where

$$\begin{aligned} &\bar{\boldsymbol{\phi}}^T(x_1(k), x_2(k)) = \\ &\begin{pmatrix} x_1(k) & x_1^3(k) & \cdots & x_1^{2\bar{L}_1+1}(k) & x_2(k) & x_1^2(k)\, x_2(k) & \cdots & x_1^{2\bar{L}_2}(k)\, x_2(k) \end{pmatrix} \end{aligned} \tag{34}$$

and the parameter vector $\bar{\boldsymbol{\theta}}$ is given by (30).

Using $\mathcal{C}4$ and $\mathcal{C}6$ in Theorem 1 thus reduces the number of parameters required for modeling periodic signals. This is expected to increase the accuracy of the estimated model especially if the modeled signal fulfills Liénard's equation.

Remark 5. The reduction in the number of parameters has a great importance in two cases. First when the modeled signal is highly corrupted with noise, *i.e.* the signal to noise ratio (SNR) is small, more inaccurate models are expected as the number of parameters increases. This is shown later in the numerical examples. A second case is when the modeled signal fullfils Liénard's equation with a high polynomial order. Hence, the dimension of the parameter vector using general approaches will be of high order and this is expected to reduce the accuracy of the estimated model significantly. It may also leads to convergence problem for the EKF estimation algorithm.

Example 1. Consider the following model with $\bar{L}_1 = 0$ and $\bar{L}_2 = 1$, *i.e.*

$$g(x_1, \bar{\boldsymbol{\theta}}_{\mathbf{1}}) = \bar{\theta}_{1,0} x_1(t) \tag{35}$$

$$f(x_1, \bar{\boldsymbol{\theta}}_{\mathbf{2}}) = \bar{\theta}_{2,0} + \bar{\theta}_{2,1}\ x_1^2(t) \tag{36}$$

It is clear that conditions $\mathcal{C}3$, $\mathcal{C}4$ and $\mathcal{C}6$ are satisfied. Condition $\mathcal{C}5$ gives

$$\bar{\theta}_{1,0} > 0.$$

Also $\mathcal{C}7$ gives

$$F(x_1) = x_1(t) \left(\bar{\theta}_{2,0} + \frac{1}{3}\ \bar{\theta}_{2,1}\ x_1^2(t) \right). \tag{37}$$

Thus

$$a = \sqrt{\frac{-3\bar{\theta}_{2,0}}{\bar{\theta}_{2,1}}}.$$

It is clear from (37) that $F(x_1)$ is nondecreasing for $x_1 > a$ provided $\bar{\theta}_{2,0} < 0$. This is because for $x_1 = a + \triangle x_1,\ \triangle x_1 > 0$,

$$F(x_1) = \left(\sqrt{\frac{-3\bar{\theta}_{2,0}}{\bar{\theta}_{2,1}}} + \triangle x_1 \right) \left[\bar{\theta}_{2,0} - \bar{\theta}_{2,0} \left(1 + \sqrt{\frac{\bar{\theta}_{2,1}}{-3\bar{\theta}_{2,0}}} \triangle x_1 \right)^2 \right].$$

Also from $\mathcal{C}7$

$$F(x_1) < 0 \quad \forall \quad 0 < x_1 < \sqrt{\frac{-3\bar{\theta}_{2,0}}{\bar{\theta}_{2,1}}}$$

$$F(x_1) > 0 \quad \forall \quad x_1 > \sqrt{\frac{-3\bar{\theta}_{2,0}}{\bar{\theta}_{2,1}}}$$

whenever

$$\bar{\theta}_{2,0} < 0 \quad \text{and} \quad \bar{\theta}_{2,1} > 0.$$

Finally

$$F(x_1) \to \infty \quad \text{as} \quad x_1 \to \infty$$

since for high values of $x_1(t)$

$$F(x_1) \approx \frac{1}{3}\ \bar{\theta}_{2,1}\ x_1^3(t).$$

Thus to guarantee the existence of a unique, stable limit cycle for the model (35)-(36), the parameters must satisfy

$$\bar{\theta}_{1,0} > 0, \quad \bar{\theta}_{2,0} < 0 \quad \text{and} \quad \bar{\theta}_{2,1} > 0. \qquad \blacksquare$$

Next the more general case for the parameterization (28), (29) is considered. The following lemma gives necessary conditions on $g(x_1, \bar{\boldsymbol{\theta}}_{\mathbf{1}})$ and $f(x_1, \bar{\boldsymbol{\theta}}_{\mathbf{2}})$ to guarantee the existence of a unique, stable limit cycle for general orders.

Lemma 1. Assume that the Liénard's system is given by

$$\begin{pmatrix} \dot{x}_1 \\ \dot{x}_2 \end{pmatrix} = \begin{pmatrix} x_2(t) \\ -g(x_1, \bar{\boldsymbol{\theta}}_{\mathbf{1}}) - f(x_1, \bar{\boldsymbol{\theta}}_{\mathbf{2}}) x_2 \end{pmatrix} \tag{38}$$

$$y(t) = \begin{pmatrix} 1 & 0 \end{pmatrix} \begin{pmatrix} x_1(t) \\ x_2(t) \end{pmatrix} \tag{39}$$

where the *odd* function $g(x_1, \bar{\boldsymbol{\theta}}_{\mathbf{1}})$ and the *even* function $f(x_1, \bar{\boldsymbol{\theta}}_{\mathbf{2}})$ are continuously differentiable polynomials given by

$$g(x_1, \bar{\boldsymbol{\theta}}_{\mathbf{1}}) = \bar{\theta}_{1,0} x_1 + \bar{\theta}_{1,1} x_1^3 + \cdots + \bar{\theta}_{1,\bar{L}_1} x_1^{2\bar{L}_1+1} \tag{40}$$

$$f(x_1, \bar{\boldsymbol{\theta}}_{\mathbf{2}}) = \bar{\theta}_{2,0} + \bar{\theta}_{2,1} x_1^2 + \cdots + \bar{\theta}_{2,\bar{L}_2} x_1^{2\bar{L}_2}. \tag{41}$$

Then this system has a *unique*, *stable* limit cycle encircling the origin in the phase plane if

$\mathcal{C}8$: All zeros of the polynomial

$$A(s) = \bar{\theta}_{1,0} + \bar{\theta}_{1,1}\ s + \bar{\theta}_{1,2}\ s^2 + \cdots + \bar{\theta}_{1,\bar{L}_1}\ s^{\bar{L}_1} \tag{42}$$

are in the LHP.

$\mathcal{C}9$: The polynomial

$$B(s) = \bar{\theta}_{2,0} + \frac{\bar{\theta}_{2,1}}{3}\ s + \frac{\bar{\theta}_{2,2}}{5}\ s^2 + \cdots + \frac{\bar{\theta}_{2,\bar{L}_2}}{2\bar{L}_2 + 1}\ s^{\bar{L}_2} \tag{43}$$

has exactly *one* positive real zero (say at a^2) and $\bar{\theta}_{2,0} < 0$.

$\mathcal{C}10$: $f(x_1, \bar{\boldsymbol{\theta}}_{\mathbf{2}}) \geq 0 \quad \forall \quad x_1 > a$.

Proof. First note that $\mathcal{C}3$, $\mathcal{C}4$ and $\mathcal{C}6$ are true by construction. It then remains to verify $\mathcal{C}5$ and $\mathcal{C}7$. Beginning with $\mathcal{C}5$, the odd function $g(x_1, \bar{\boldsymbol{\theta}}_{\mathbf{1}})$ can be written as

$$g(x_1, \bar{\boldsymbol{\theta}}_{\mathbf{1}}) = x_1\ A(x_1^2) \tag{44}$$

Choosing $s = x_1^2$ gives (42). Further $g(x_1) > 0\ \forall\ x_1 > 0$ if $A(x_1^2) > 0$. The latter is the case if all zeros of $A(s)$ are in the LHP, since for negative zeros $A(s)$ takes the form

$$A(s) = \prod_{i=1}^{\bar{L}_1} (s + z_i) \quad \text{for} \quad z_i > 0 \tag{45}$$

where $-z_i, i = 1, \cdots, \bar{L}_1$ are the zeros of $A(s)$. Thus $\mathcal{C}8$ implies $\mathcal{C}5$.

Proceeding with $\mathcal{C}7$, since $f(x_1, \bar{\boldsymbol{\theta}}_{\boldsymbol{2}})$ is an even function

$$F(x_1) = x_1 \; B(x_1^2). \tag{46}$$

To satisfy condition $\mathcal{C}7$, $B(x_1^2)$ should have exactly one positive zero at $x_1 = a$, be negative for $0 < x_1 < a$, be positive and nondecreasing for $x_1 > a$, and $F(x_1) \to \infty$ as $x_1 \to \infty$. This means $\bar{\theta}_{2,0}$ should be negative and $B(s)$ given by (43) should have exactly one positive real zero. The nondecreasing condition on $F(x_1)$ for $x_1 > a$ means $\frac{dF}{dx_1} \geq 0$ for $x_1 > a$. Since $F(x_1) = \int_0^{x_1} f(u)du$, differentiating both sides gives $\frac{dF}{dx_1} = f(x_1, \bar{\boldsymbol{\theta}}_{\boldsymbol{2}})$. Thus $F(x_1)$ is a nondecreasing function if $\mathcal{C}10$ satisfied. Hence $\mathcal{C}9$ and $\mathcal{C}10$ together imply $\mathcal{C}7$. ■

Remark 6. From Routh's stability criterion for continuous systems, all zeros of $A(s)$ are in the LHP if there are no sign changes in the left-most column of the Routh array, see [16]. A necessary but not sufficient condition for this to happen is $\bar{\theta}_{1,i} > 0$ for $i = 0, \cdots, \bar{L}_1$. Also from Descarte's rule of sign, see [17], the number of positive real roots of $B(s)$ is either equal to the number of variations of sign between successive terms in $B(s)$ when arranged in descending powers of s or less than that number by an even integer. Thus $B(s)$ should have an odd number of sign variations.

In addition to the reduction achieved in the number of parameters to model periodic signals, another advantage of the approach used in this paper can be concluded from Lemma 1. Since Lemma 1 gives more specific conditions on the parameters, these conditions can be used as a detection method for the existence of a unique, stable periodic orbit that models the periodic signal under investigation. Once the parameter vector $\bar{\boldsymbol{\theta}}$ is estimated, the polynomials $A(s)$ and $B(s)$ given by (42) and (43) can be constructed and the conditions of Lemma 1 can be examined. These findings are further explained in the examples of Section 4.

Remark 7. Imposing the constraints of Lemma 1 on the parameters during the estimation process is complicated and not so useful. This is so because the optimization problem will have degrees of freedom equals to the number of parameters which is most probably higher than 2. In this case one can not expect to get more accurate parameter estimates by imposing the constraints during the estimation phase. On the other hand to examine the conditions of Lemma 1 as a validation phase is easy as shown later in the numerical examples.

Remark 8. Note that there may be unique periodic solutions even in cases where the parameter constraints are not fulfilled. This is because the conditions of Theorem 1 are only sufficient for general periodic signals, and necessary for signals that fulfills Liénard's system description.

4 Numerical examples

In this section a comparative simulation study for the two modeling approaches (7) and (11) is presented. First the two approaches were used to model a periodic signal

generated by Liénard's equation. Then the two approaches were tested for modeling a periodic signal that does not fulfill Liénard's equation description. Finally, Monte Carlo experiments were performed on the two modeling approaches to study the statistical properties of the parameter estimates with respect to SNR and data length.

Example 2. In this example the data were generated using the following Liénard's system

$$\begin{pmatrix} \dot{x}_1 \\ \dot{x}_2 \end{pmatrix} = \begin{pmatrix} x_2 \\ -x_1 + (1 - 2\ x_1^4)\ x_2 \end{pmatrix} \tag{47}$$

which satisfies the conditions of Theorem 1. The Matlab routine `ode45` was used to solve (47). The initial states of (47) were selected as $(x_1(0) \quad x_2(0))^T = (1 \quad 0)^T$. All results below are based on data runs of length $N = 3 \times 10^4$ samples with a sampling interval $T_S = 0.01$ s. The period of the solution of (47) is approximately 7 seconds. Hence, about 40 periods of the signal are measured with approximately 700 samples per period. The measured signal was selected as the first state with white Gaussian noise added to obtain data with a signal to noise ratio of 30 dB.

The model (7) is compared with the model (11) by modeling the periodic signal generated by (47) using the EKF estimation algorithm introduced in [9]. The two EKF algorithms were initialized with

$$(\widehat{x}_1(0) \quad \widehat{x}_2(0) \quad \widehat{\bar{\boldsymbol{\theta}}}^T(0))^T = (-0.5 \quad 0.5 \quad \mathbf{0})^T$$

$$(\widehat{x}_1(0) \quad \widehat{x}_2(0) \quad \widehat{\bar{\boldsymbol{\theta}}}^T(0))^T = (-0.5 \quad 0.5 \quad \mathbf{0})^T.$$

The remaining parameters were selected as $\boldsymbol{P}(0) = 10\boldsymbol{I}$, $\boldsymbol{R}_1 = 0.001\boldsymbol{I}$ and $R_2 = 1$. The orders of the models were chosen as $L = 4$, $M = 1$, $\bar{L}_1 = 0$ and $\bar{L}_2 = 2$. The number of estimated parameters was $(L + 1)(M + 1) = 10$ for the model (7) and $\bar{L}_1 + \bar{L}_2 + 2 = 4$ for the model (11).

After 3×10^4 samples the parameter estimates were as follows:

$$\widehat{\bar{\boldsymbol{\theta}}}^T = (0.005, 1.021, -1.149, -0.009, 0.008, -0.235, 0.086, 0.020, -0.011, -1.908)$$

$$\widehat{\bar{\boldsymbol{\theta}}}^T = (1.036, -0.990, 0.040, 2.102)$$

Note the negative sign difference between $\widehat{\boldsymbol{\theta}}$ and $\widehat{\bar{\boldsymbol{\theta}}}$, *c.f.* (22) and (33). Comparing the estimated parameter vector $\widehat{\bar{\boldsymbol{\theta}}}$ with the results of Lemma 1 gives $\bar{\theta}_{1,0} = 1.036 > 0$, $\bar{\theta}_{2,0} = -0.99 < 0$ and $\bar{\theta}_{2,2} = 2.102$. Thus $A(s) = 1.036$ and $B(s) = -0.99 + \frac{2.102}{5}\ s^2$. It is clear that $A(s)$ does not have zeros in the RHP and $B(s)$ has one positive zero at 1.535. Also $f(x_1, \bar{\boldsymbol{\theta}}_{\mathbf{2}}) = 2.102x_1^4 - 0.99 > 0\ \forall x_1 > \sqrt{1.535}$. This shows that the estimated model represents a unique, stable periodic orbit surrounding the origin in the phase plane.

The parameter estimates and phase plots for the system (47) and the estimated models are shown in Figures 1-3. The results indicate that the reduction in the number of estimated parameters achieved using models based on Liénard's systems significantly increases the accuracy of the estimated models.

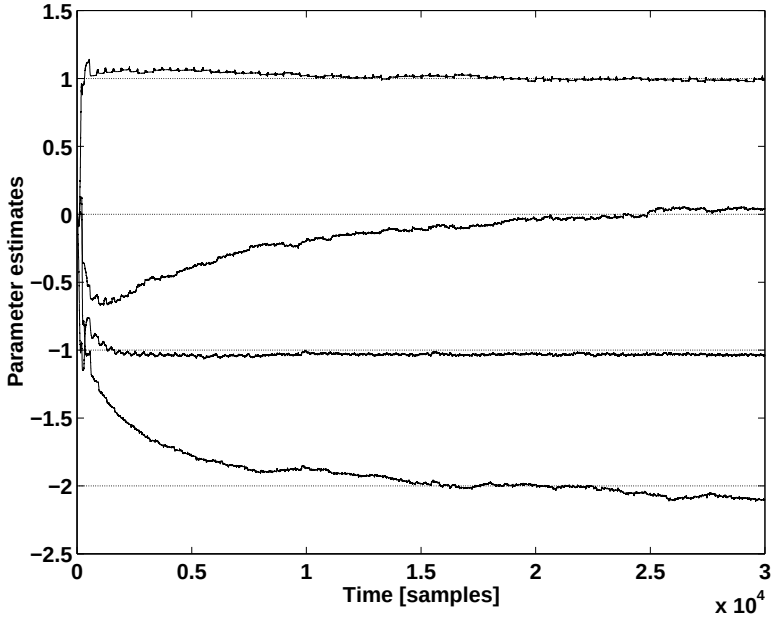

Figure 1: Parameter convergence for the model (11).

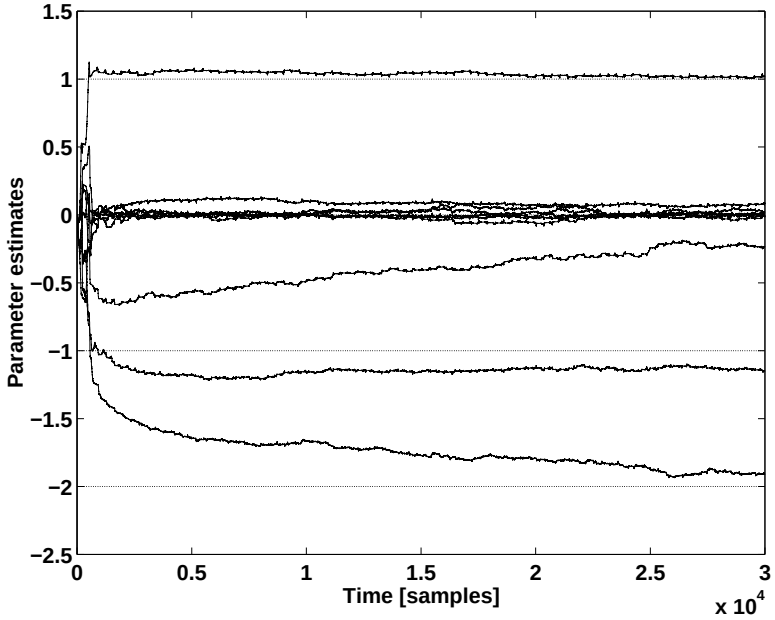

Figure 2: Parameter convergence for the model (7).

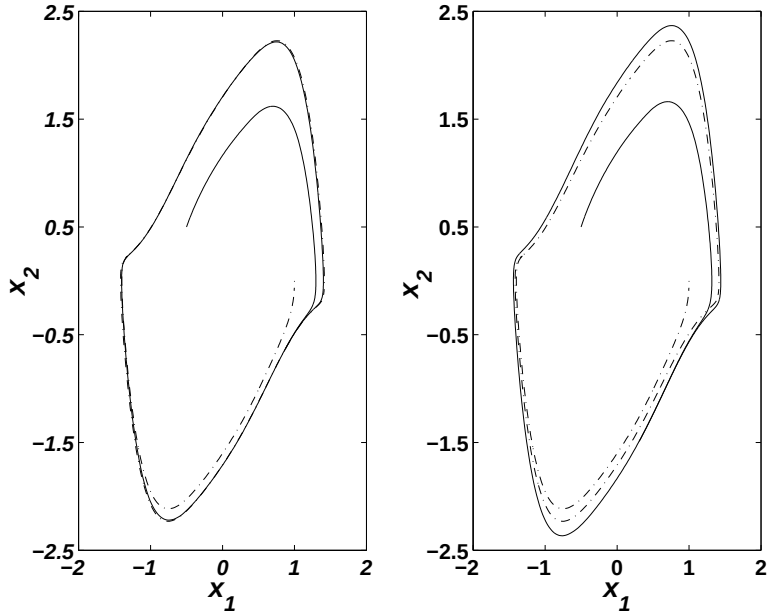

Figure 3: True (dashed) and estimated (solid) phase plane plots for system (47). Model (11) left, model (7) right. The models are initialized as $x_1(0) = -0.5$, $x_2(0) = 0.5$ and the final parameter estimate $\widehat{\bar{\boldsymbol{\theta}}}$ or $\widehat{\bar{\boldsymbol{\theta}}}$, respectively, is applied.

Example 3. Consider the following system

$$\begin{pmatrix} \dot{x}_1 \\ \dot{x}_2 \end{pmatrix} = \begin{pmatrix} x_2 \\ -x_1 + (1 - 3\ x_1^2 - 2\ x_2^2)\ x_2 \end{pmatrix} \tag{48}$$

which does not match Liénard's system description. Similarly as done in Example 2, 3×10^4 samples were generated from (48) with $T_S = 0.01$ s. The period of the solution of (48) is approximately 6 seconds. Hence, about 50 periods of the signal are measured with approximately 600 samples per period.

The model (7) is compared with the model (11) by modeling the periodic signal generated by (48) using the EKF estimation algorithm. The two EKF algorithms were initialized as done in Example 2 except that $\boldsymbol{P}(0) = 10000\boldsymbol{I}$. The orders of the models were chosen as $L = 2$, $M = 3$, $\bar{L}_1 = 0$ and $\bar{L}_2 = 1$. The number of estimated parameters was 12 for the model (7) and 3 for the model (11).

The phase plots for the system (48) and the estimated models are shown in Figure 4. The results show that even if the modeled signal does not fulfill Liénard's equation, the underparameterized model (11) still represents a unique and stable periodic orbit that slightly deviates from the true periodic orbit and the estimated periodic orbit using the model (7) with the correct polynomial orders.

Example 4. In this example 100 Monte Carlo simulations were performed on the system (47) to study the performance of the two modeling approaches (7) and (11) compared to the Cramér-Rao bound (CRB) derived in [18] with different noise realiza-

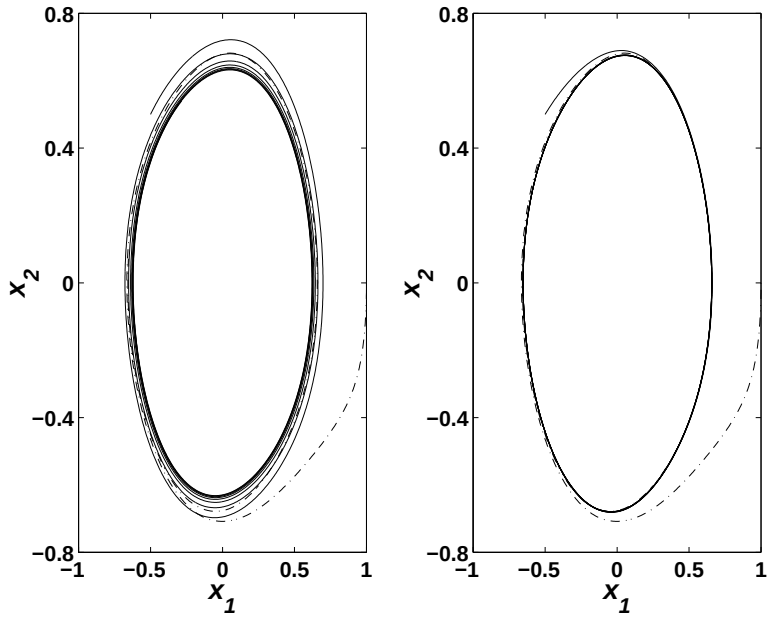

Figure 4: True (dashed) and estimated (solid) phase plane plots for system (48). Model (11) left, model (7) right. The models are initialized as $x_1(0) = -0.5$, $x_2(0) = 0.5$ and the final parameter estimate $\hat{\tilde{\boldsymbol{\theta}}}$ or $\hat{\bar{\boldsymbol{\theta}}}$, respectively, is applied.

tions. The data were generated as done in Example 2. The two EKF algorithms were initialized with

$$(\hat{x}_1(0) \quad \hat{x}_2(0) \quad \hat{\tilde{\boldsymbol{\theta}}}^T(0))^T = (-0.5 \quad 0.5 \quad \tilde{\boldsymbol{\theta}}_o + \tilde{\boldsymbol{\sigma}})^T$$

$$(\hat{x}_1(0) \quad \hat{x}_2(0) \quad \hat{\bar{\boldsymbol{\theta}}}^T(0))^T = (-0.5 \quad 0.5 \quad \bar{\boldsymbol{\theta}}_o + \bar{\boldsymbol{\sigma}})^T.$$

where $\tilde{\boldsymbol{\theta}}_o$ and $\bar{\boldsymbol{\theta}}_o$ are the true parameter vectors, $\tilde{\boldsymbol{\sigma}}$ and $\bar{\boldsymbol{\sigma}}$ are the standard deviation as predicted by the CRB. The remaining parameters were selected as $\boldsymbol{P}(0) = 10^{-4}\boldsymbol{I}$, $\boldsymbol{R}_1 = 10^{-6}\boldsymbol{I}$ and $R_2 = 1$. The orders of the models were chosen as $L = 4$, $M = 1$, $\bar{L}_1 = 0$ and $\bar{L}_2 = 2$.

The mean square error (MSE) of the estimated parameter vector and the CRB were evaluated for $N = 3 \times 10^4$ samples with different signal to noise ratios (SNR). The results are shown in Figures 5-7. Also as a measure of performance,

$$V_1 = \frac{1}{n}\sum_{1}^{n} \|\hat{\tilde{\boldsymbol{\theta}}}_N - \tilde{\boldsymbol{\theta}}_o\|_2 \tag{49}$$

$$V_2 = \frac{1}{n}\sum_{1}^{n} \|\hat{\bar{\boldsymbol{\theta}}}_N - \bar{\boldsymbol{\theta}}_o\|_2 \tag{50}$$

were computed and plotted as a function of the SNR in Fig. 8 (n is the number of experiments in which convergence to the true parameter vector is achieved). Also, the

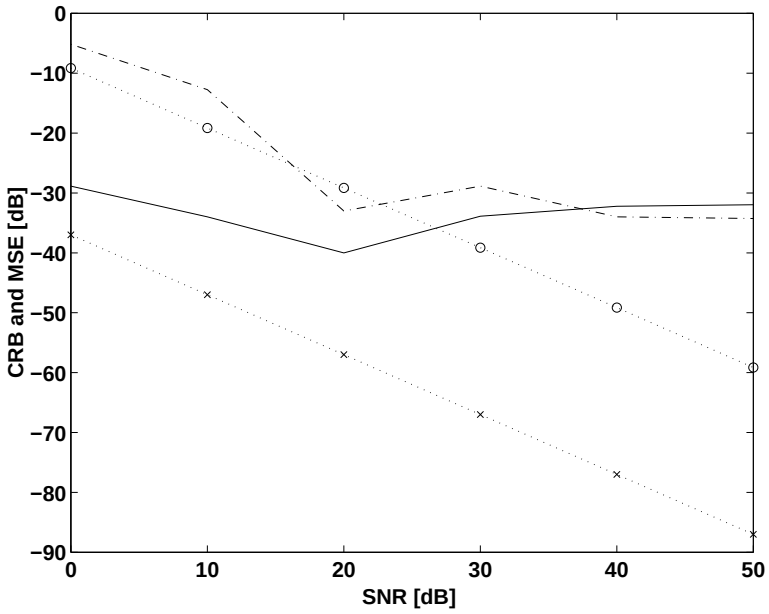

Figure 5: The MSE for $\tilde{\theta}_{1,0}$ (dashed) and $\bar{\theta}_{1,0}$ (solid) compared to the CRB of $\tilde{\theta}$ (dot-o) and $\bar{\theta}$ (dot-x) [$N = 3 \times 10^4$ samples].

Monte-Carlo experiments were repeated for different data length with SNR=10 dB and SNR=30 dB. The initial values of $\boldsymbol{P}$ and $\boldsymbol{R_1}$ were chosen as $\boldsymbol{P}(0) = 10\boldsymbol{I}$, $\boldsymbol{R}_1 = 10^{-5}\boldsymbol{I}$. The results are shown in Figures 9-16. The results show that the approach of this paper gives significantly better parameter estimates compared to the approach (7) especially for small signal to noise ratios.

5 Conclusions

The modeling of periodic signals using Liénard's equation has been studied. The approach of this paper is based on using the appropriate assumptions imposed in Liénard's theorem to guarantee the existence of a unique and stable periodic orbit in the phase plane surrounding the origin. Using these conditions leads to a reduction in the model parameters. This reduction not only reduces the computational load but also significantly increases the accuracy of the model in case the periodic signal does fulfill Liénard's equation description compared to more general approaches. Moreover, the approach can be used for modeling signals that do not fulfill Liénard's equation with only a small degradation in the accuracy of the estimated models.

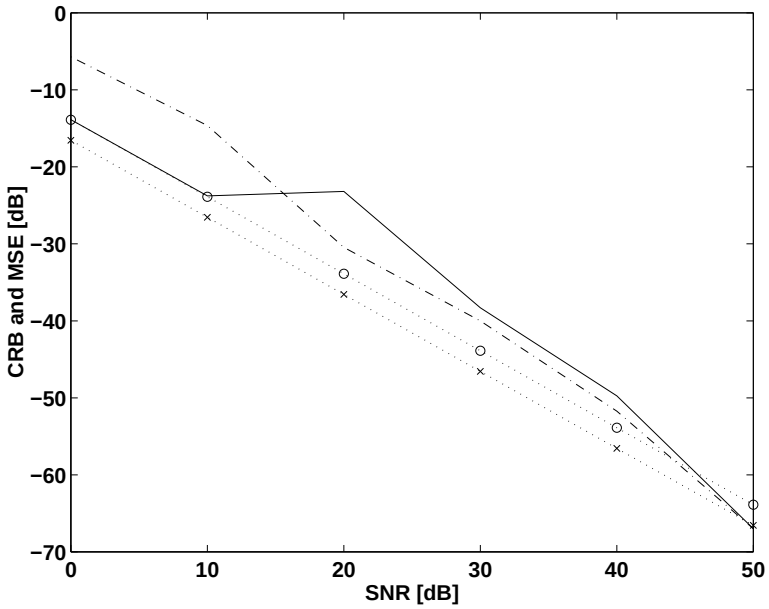

Figure 6: The MSE for $\tilde{\theta}_{0,1}$ (dashed) and $\bar{\theta}_{2,0}$ (solid) compared to the CRB of $\tilde{\theta}$ (dot-o) and $\bar{\theta}$ (dot-x) [$N = 3 \times 10^4$ samples].

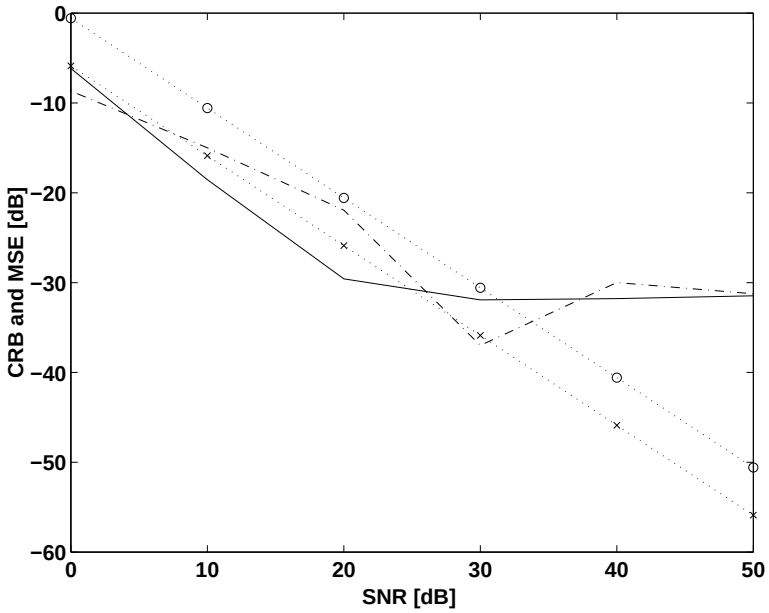

Figure 7: The MSE for $\tilde{\theta}_{4,1}$ (dashed) and $\bar{\theta}_{2,2}$ (solid) compared to the CRB of $\tilde{\theta}$ (dot-o) and $\bar{\theta}$ (dot-x) [$N = 3 \times 10^4$ samples].

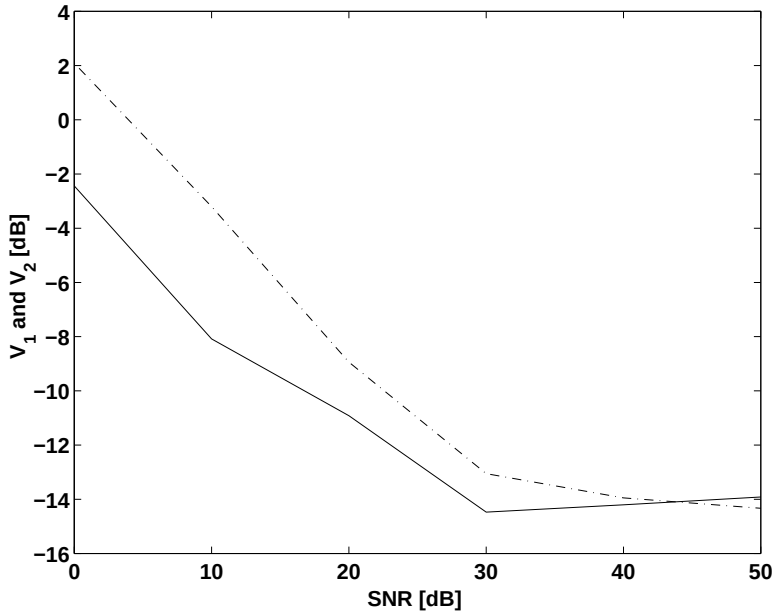

Figure 8: V_1 (dashed) and V_2 (solid) with SNR [$N = 3 \times 10^4$ samples].

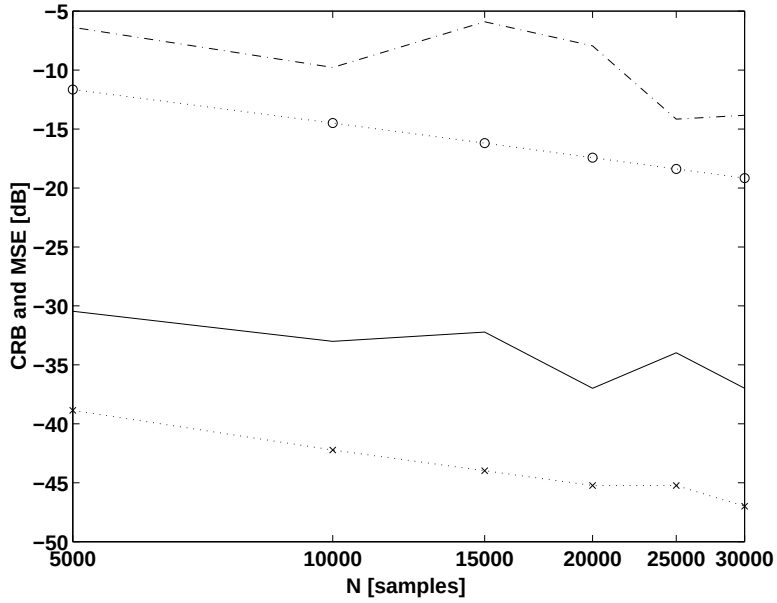

Figure 9: The MSE for $\tilde{\theta}_{1,0}$ (dashed) and $\bar{\theta}_{1,0}$ (solid) compared to the CRB of $\tilde{\theta}$ (dot-o) and $\bar{\theta}$ (dot-x) [SNR=10 dB].

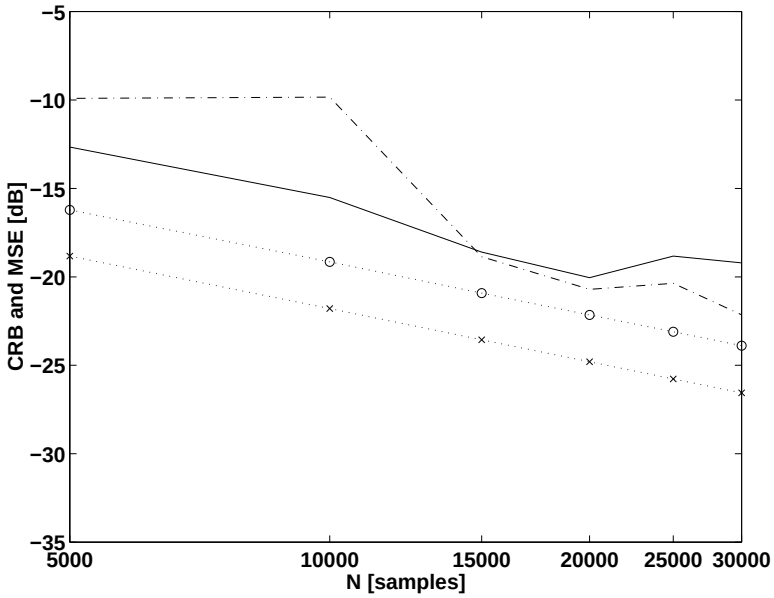

Figure 10: The MSE for $\tilde{\theta}_{0,1}$ (dashed) and $\bar{\theta}_{2,0}$ (solid) compared to the CRB of $\tilde{\theta}$ (dot-o) and $\bar{\theta}$ (dot-x) [SNR=10 dB].

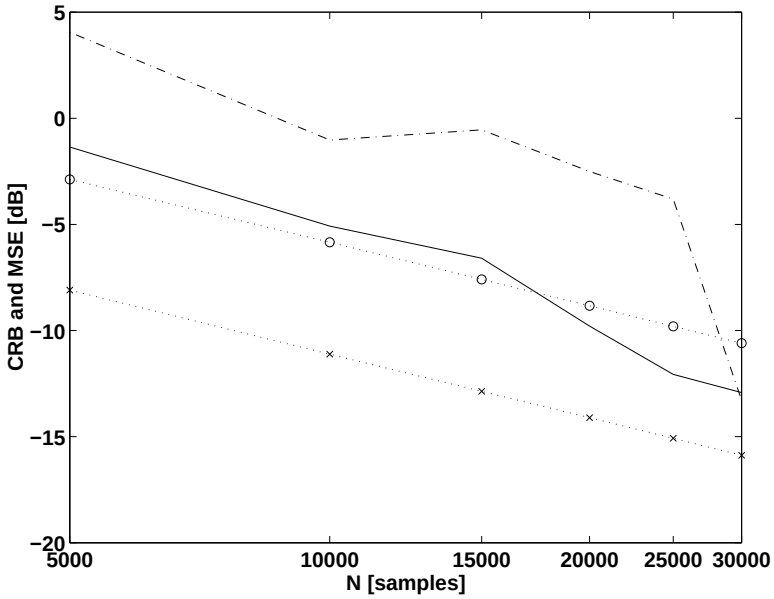

Figure 11: The MSE for $\tilde{\theta}_{4,1}$ (dashed) and $\bar{\theta}_{2,2}$ (solid) compared to the CRB of $\tilde{\theta}$ (dot-o) and $\bar{\theta}$ (dot-x) [SNR=10 dB].

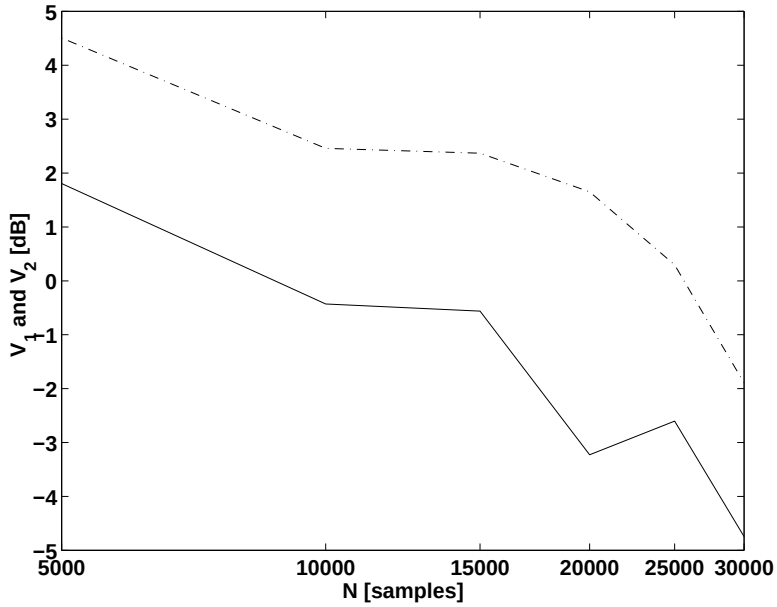

Figure 12: V_1 (dashed) and V_2 (solid) with N [SNR=10 dB].

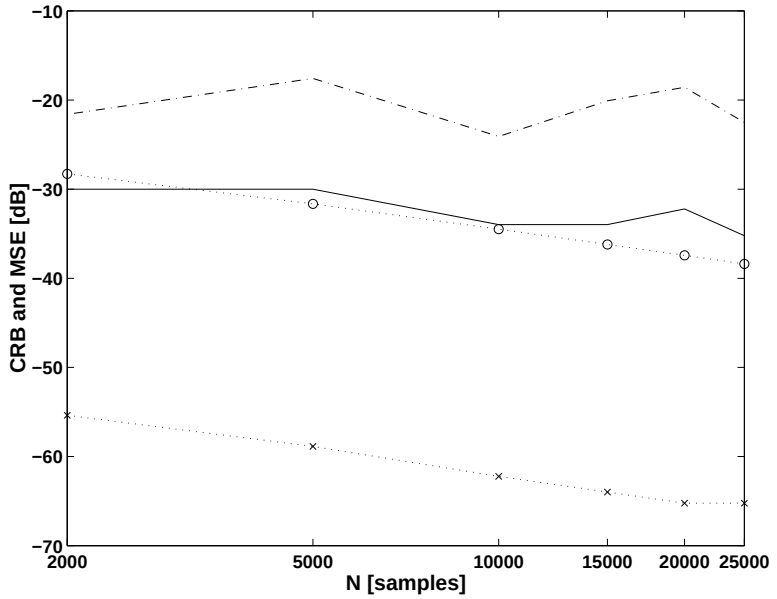

Figure 13: The MSE for $\tilde{\theta}_{1,0}$ (dashed) and $\bar{\theta}_{1,0}$ (solid) compared to the CRB of $\tilde{\theta}$ (dot-o) and $\bar{\theta}$ (dot-x) [SNR=30 dB].

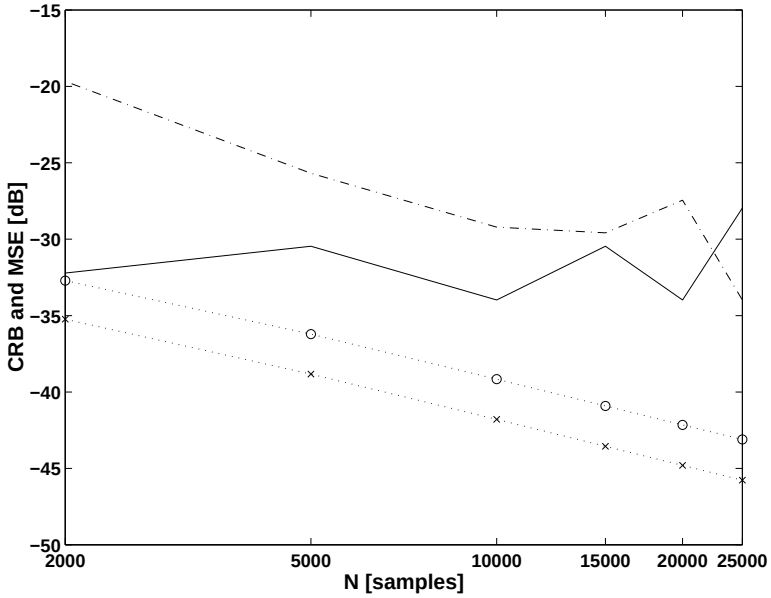

Figure 14: The MSE for $\tilde{\theta}_{0,1}$ (dashed) and $\bar{\theta}_{2,0}$ (solid) compared to the CRB of $\tilde{\theta}$ (dot-o) and $\bar{\theta}$ (dot-x) [SNR=30 dB].

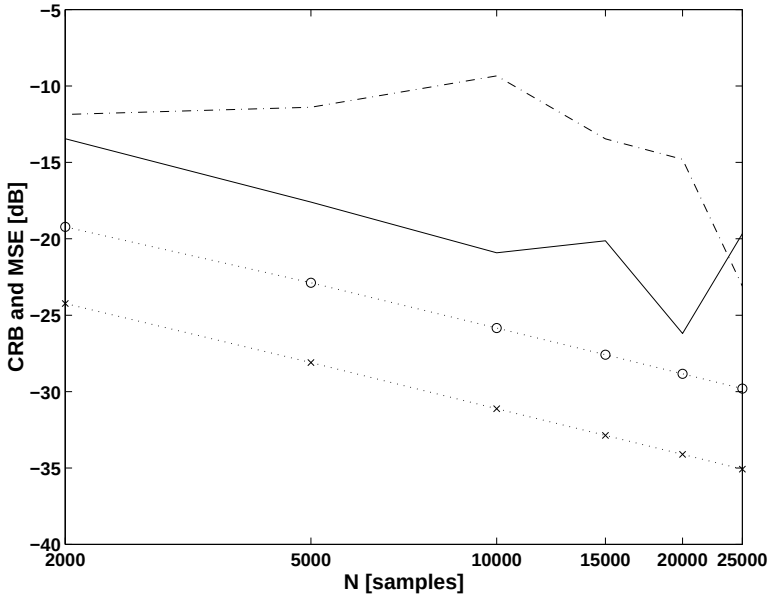

Figure 15: The MSE for $\tilde{\theta}_{4,1}$ (dashed) and $\bar{\theta}_{2,2}$ (solid) compared to the CRB of $\tilde{\theta}$ (dot-o) and $\bar{\theta}$ (dot-x) [SNR=30 dB].

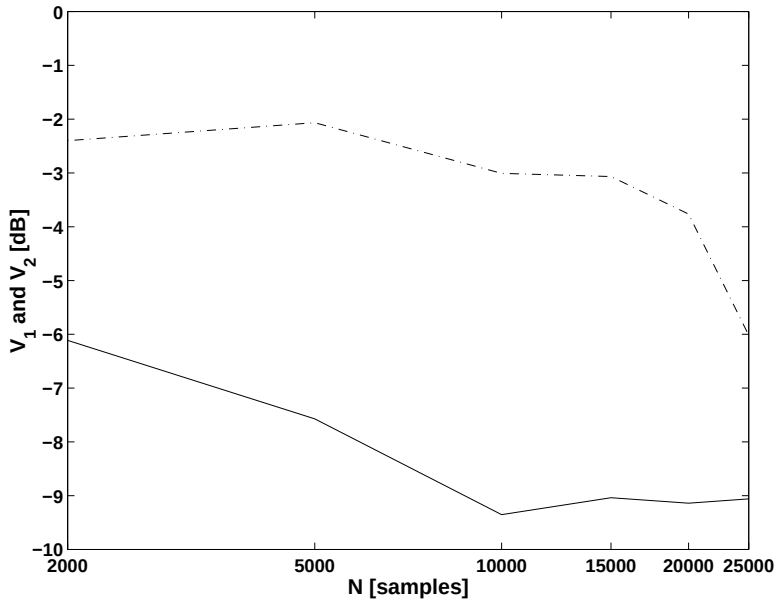

Figure 16: V_1 (dashed) and V_2 (solid) with N [SNR=30 dB].

References

[1] P. Stoica and R. Moses, *Introduction to Spectral Analysis*, Prentice-Hall, Upper Saddle River, NJ, USA, 1997.

[2] A. Nehorai and B. Porat, "Adaptive comb filtering for harmonic signal enhancement," *IEEE Transactions on Acoustics, Speech, and Signal Processing*, vol. ASSP-34, pp. 1124–1138, 1986.

[3] T. Wigren and P. Händel, "Harmonic signal modeling using adaptive nonlinear function estimation," in *Proc. of IEEE International Conference on Acoustics, Speech and Signal Processing*, Atlanta, GA, May, 7–10, 1996.

[4] E. Abd-Elrady, *Harmonic Signal Modeling Based on the Wiener Model Structure*, Licentiate thesis, Department of Systems and Control, Uppsala University, Uppsala, Sweden, 2002.

[5] H. K. Khalil, *Nonlinear Systems*, Prentice-Hall, Upper Saddle River, NJ, USA, third edition, 2002.

[6] L. Perko, *Differential Equations and Dynamical Systems*, Texts in Applied Mathematics. Springer-Verlag, NY, USA, 1991.

[7] D. W. Jordan and P. Smith, *Nonlinear Ordinary Differential Equations: An Introduction to Dynamical Systems*, Oxford University Press, Oxford, UK, third edition, 1999.

[8] M. Vidyasagar, *Nonlinear Systems Analysis*, Prentice Hall, Englewood Cliffs, NJ, USA, second edition, 1993.

[9] T. Wigren, E. Abd-Elrady, and T. Söderström, "Harmonic signal analysis with Kalman filters using periodic orbits of nonlinear ODEs," in *Proc. of IEEE International Conference on Acoustics, Speech, and Signal Processing*, Hong Kong, April, 6–10, 2003.

[10] T. Wigren, E. Abd-Elrady, and T. Söderström, "Least squares harmonic signal analysis using periodic orbits of ODEs," in *Proc. of 13th IFAC Symposium on System Identification*, Rotterdam, Netherlands, August, 27–29, 2003.

[11] E. Abd-Elrady, T. Söderström, and T. Wigren, "Periodic signal analysis using orbits of nonlinear ODEs based on the Markov estimate," *In preparation*, 2003.

[12] S. H. Strogatz, *Nonlinear Dynamics and Chaos With Applications to Physics, Biology, Chemistry, and Engineering*, Addison-Wesley, 1994.

[13] H. N. Moreira, "Liénard-type equations and the epidemiology of malaria," *Ecological Modelling*, vol. 60, pp. 139–150, 1992.

[14] T. Wigren and T. Söderström, "Second order ODEs are sufficent for modeling of many periodic signals," Tech. Rep. 2003-025, Information Technology, Uppsala University, Uppsala, Sweden, 2003.

[15] B. Carlsson, *Digital Differentiating Filters and Model Based Fault Detection*, Ph.D. thesis, Department of Technology, Uppsala University, Uppsala, Sweden, 1989.

[16] K. Ogata, *Modern Control Engineering*, Prentice Hall, Upper Saddle River, NJ, USA, fourth edition, 2002.

[17] E. I. Jury, *Inners and Stability of Dynamic Systems*, Wiley-Interscience, 1974.

[18] T. Söderström, T. Wigren, and E. Abd-Elrady, "Periodic signal analysis by maximum likelihood modeling of orbits of nonlinear ODEs," *In preparation*, 2003.